

# Comparative Degradation of C. I. Acid Green 25 and C. I. Basic Blue 9 by Electrochemical, Photoelectrochemical and Photocatalytic Oxidation Methods

Rafał Sałata<sup>1</sup>, Katarzyna Siwińska – Stefańska<sup>2</sup>, Jolanta Sokółowska<sup>1,\*</sup>

<sup>1</sup> Institute of Polymer and Dye Technology, Lodz University of Technology, Stefanowskiego 12/16, 90-924 Lodz, Poland

<sup>2</sup> Institute of Chemical Technology and Engineering, Poznan University of Technology, Berdychowo 4, 61-131 Poznan, Poland

\*E-mail: [jsokolow@p.lodz.pl](mailto:jsokolow@p.lodz.pl)

Received: 4 June 2018 / Accepted: 6 November 2018 / Published: 30 November 2018

---

The electrochemical, photoelectrochemical, and photocatalytic degradation of C. I. Acid Green 25 (AG) and C. I. Basic Blue 9 (Methylene Blue, MB) was investigated. For the electrochemical and photoelectrochemical oxidation, a titanium electrode coated with a mixture of TiO<sub>2</sub>/RuO<sub>2</sub> was employed. In the photocatalytic degradation, Pt/P25 catalysts containing different amounts of platinum were used. The highest effectiveness of C. I. Acid Green 25 conversion (up to 90% based on TOC and up to 96% based on COD) was achieved using the photocatalytic method with the application of Pt/P25 catalyst (ca. 0.50 wt.% of Pt). The photoassisted electrolysis of C. I. Basic Blue 9 gave a comparable conversion (based on TOC ~ 86%) to that obtained with Pt/P25 photocatalytic treatment (based on TOC ~ 89%) in which a very small increase in the decolourisation rate constant over P25 alone was noted.

---

**Keywords:** Electrochemical oxidation, photoelectrochemical oxidation, photocatalytic oxidation, TiO<sub>2</sub>, organic dyes, water treatment.

## 1. INTRODUCTION

For many years, textile, food, printing, and cosmetics industries have been the main causes of water pollution with organic compounds, mainly dyes [1]. Most of them are non-biodegradable, which poses a serious problem to public health. Therefore, the complete degradation and mineralisation of pollutants [2, 3] is an important goal.

Heterogeneous photocatalysis is a promising technology, because it eliminates the disadvantages of conventional methods, such as a narrow spectrum of application, or the generation of large amounts

of sludge [4]. In addition, the use of photocatalytic methods leads, in most cases to almost complete conversion of organic compounds into carbon dioxide and water. Among many catalysts,  $\text{TiO}_2$  seems to be interesting from a green chemistry point of view because of environmental safety, low cost, and chemical stability. Additionally, the improvement of its activity often involves surface modification [5]. The simplest method is mixing anatase and rutile phase, but the highest mineralisation is usually obtained by doping the semiconductor with noble metals [6]. However, even small amounts of dopant, such as gold, platinum, or silver, increases the cost of catalysts [7-9]. The development that has taken place in the photocatalytic degradation of organic dyes over the last 30 years suggests that this problem will be solved [10].

Another effective method is electrochemical water treatment [11,12]. Over the years, electrochemical oxidation of organic waste has received much attention due to its attractive characteristics of energy efficiency, possibility of automation, and versatility [13]. For colour removal, while many different anodes such as lead, platinum, graphite, and lead dioxide can be used, titanium anodes coated with metal oxides (titanium or ruthenium) have been found to be very effective [14, 15].

The purpose of this study is to evaluate the optimal conditions and procedures to achieve the highest mineralisation of organic dyes. This paper details the application of electrochemical, photoelectrochemical and photocatalytic techniques for the degradation of C. I. Acid Green 25 and C. I. Basic Blue 9 (Figure 1). In the electrochemical method, a titanium electrode coated with a mixture of titanium and ruthenium oxides (70%/30%) was used. It is well known that  $\text{RuO}_2$  shows metallic conductivity and electrocatalytic activity, whereas  $\text{TiO}_2$  is a photochemically active semiconductor. In the photocatalytic method, Pt/P25 catalysts with different platinum contents were applied.

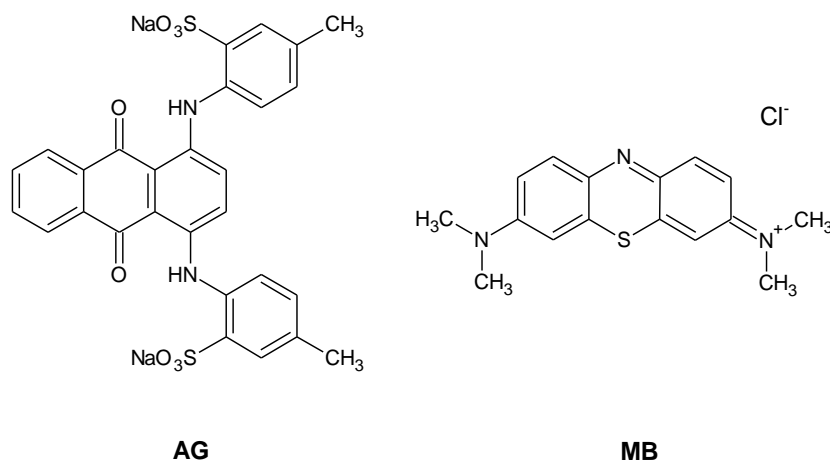


**Figure 1.** C. I. Acid Green 25 (AG) and C. I. Basic Blue 9 (MB)

## 2. EXPERIMENTAL

### 2.1 Reagents and materials

Aeroxide® P25 (surface area 35-65m<sup>2</sup> g<sup>-1</sup>, 21nm particle size, ≥99.5% trace metal basic), chloroplatinic acid hexahydrate, C. I. Acid Green 25 and C. I. Basic Blue 9 were purchased from Sigma-

Aldrich (Poznan, Poland). All reagents used were analytical grade. C. I. Acid Green 25 and C. I. Basic Blue 9 solutions were prepared by dissolving the substrate in 0.1 mol NaClO<sub>4</sub> (Fluka) or 0.1 mol KCl (Sigma-Aldrich), respectively. Solutions of the dyes were prepared using doubly distilled water. H<sub>2</sub>SO<sub>4</sub> was purchased from Chempur, Poland. Ag<sub>2</sub>SO<sub>4</sub>, K<sub>2</sub>Cr<sub>2</sub>O<sub>7</sub> and Fe(NH<sub>4</sub>)<sub>2</sub>(SO<sub>4</sub>)<sub>2</sub> were purchased from POCh Gliwice, Poland.

## 2.2 Electrochemical and photoelectrochemical experiments

Cyclic voltammetry (CV) [16, 17] and differential pulse voltammetry (DPV) methods were used in electrochemical measurements carried out in an Autolab PGSTAT 30 Electrochemical Analyser (EcoChemie, Netherlands). A three-electrode cell was used in all experiments. A titanium electrode coated with TiO<sub>2</sub>/RuO<sub>2</sub> (97%/3% or 70%/30%) was used as the anode (obtained from the Department of Inorganic Chemistry and Technology of Silesian Technical University), and a platinum electrode was used as a working electrode (geometric surface area of 0.5 cm<sup>2</sup>). The cathode was a platinum electrode. The potential of the working electrode was measured using a saturated calomel electrode (SCE). Before measurements, the solutions were purged with argon in order to remove dissolved oxygen. During measurements, an argon blanket was kept over the solutions. All experiments were carried out at room temperature. Peak potential ( $E_{pa}$ ), the potential at which the current is half of the peak value ( $E_{pa/2}$ ) and the half-wave potential ( $E_{1/2}$ ) for the first step of the C. I. Acid Green 25 and C. I. Basic Blue 9 electrooxidations were determined from recorded voltammograms. The anodic transition coefficient ( $\beta n_\beta$ ) and heterogeneous rate constant ( $k_{bh}$ ) at the half-wave potential ( $E_{1/2}$ ) were calculated from the following equations [17]:

$$\beta n_\beta = \frac{1.857RT}{F(E_{pa} - E_{pa/2})} \quad (1)$$

$$E_{pa} = -1.14 \frac{RT}{\beta n_\beta F} - \frac{RT}{\beta n_\beta F} \ln \frac{k_{bh}^0}{D_{red}^{1/2}} + \frac{RT}{2\beta n_\beta F} \ln \beta n_\beta v \quad (2)$$

$$k_{bh} = k_{bh}^0 \exp\left(\frac{-\beta n_\beta FE}{RT}\right) \quad (3)$$

where:  $D_{red}$  – diffusion coefficient of reduced form, cm<sup>2</sup> s<sup>-1</sup>,

$v$  – scan rate, V s<sup>-1</sup>,

$F$  – Faraday constant (96,487 C mol<sup>-1</sup>),

$R$  – universal gas constant (8.314 J K<sup>-1</sup> mol<sup>-1</sup>),

$T$  – Kelvin temperature (K),

$k_{bh}^0$  – heterogeneous rate constant at a peak potential vs. SCE (cm s<sup>-1</sup>),

$i_a$  – anodic current intensity (A cm<sup>-2</sup>),

$E_{pa}$  – peak potential,

$E_{pa/2}$  – potential at which the current is half of the peak value

Preparative oxidation of the dyes was carried out in an electrochemical quartz cell with undivided electrode compartments under galvanostatic conditions. A current intensity of 0.4 A was used at the electrode surface of 20 cm<sup>2</sup>, which corresponds to the current density of 2.0 × 10<sup>-2</sup> A cm<sup>-2</sup>. Photoelectrochemical oxidation of the dyes was carried out in the same electrochemical cell placed in the photochemical reactor (Rayonet RPR-200, Southern New England Ultraviolet Company) equipped with eight lamps emitting radiation of 254 nm (radiation intensity 11.3 mW cm<sup>-2</sup>), 300 nm (radiation intensity 6.4 mW cm<sup>-2</sup>) and 350 nm (radiation intensity 5.3 mW cm<sup>-2</sup>) for 1.5 h.

### 2.3 Analytical procedures

The conversion of the dyes was presented as a change in absorbance ( $\eta_{Abs}$ ) at  $\lambda_{max}$ , total organic carbon ( $\eta_{TOC}$ ) and chemical oxygen demand ( $\eta_{COD}$ ) according to the equations 4-6, where  $A_0$  and  $A_t$  denote the absorbance at the beginning and at time  $t$ , and  $TOC_0$ ,  $TOC_t$ ,  $COD_0$  and  $COD_t$ , refer to TOC and COD values at the beginning and at time  $t$  of the appropriate parameters, respectively.

The conversion of the dyes was presented as a change in absorbance ( $\eta_{Abs}$ ) at  $\lambda_{max}$ , total organic carbon ( $\eta_{TOC}$ ) and chemical oxygen demand ( $\eta_{COD}$ ) according to equations 4-6, where  $A_0$  and  $A_t$  denote the absorbance at the beginning and at time  $t$ , and  $TOC_0$ ,  $TOC_t$ ,  $COD_0$  and  $COD_t$  refer to the TOC and COD values at the beginning and at time  $t$  of the appropriate parameters, respectively.

$$\eta_{Abs} = \frac{A_0 - A_t}{A_0} \times 100\% \quad (4)$$

$$\eta_{TOC} = \frac{TOC_0 - TOC_t}{TOC_0} \times 100\% \quad (5)$$

$$\eta_{COD} = \frac{COD_0 - COD_t}{COD_0} \times 100\% \quad (6)$$

TOC was analysed with a TOC 5050 A Shimadzu Total Organic Carbon Analyser (Japan). COD was determined according to the procedure described in [18]. The concentration of the dyes was followed by measuring the decrease in absorbance at  $\lambda_{max}$  using a Jasco V-670 spectrophotometer (Jasco, Japan).

### 2.4 Preparation of Pt/P25

The catalysts were prepared by a photodeposition procedure as described in [19] with the exception of the applied light source – radiation of 575 nm from eight UV lamps RPR 5750 A (Southern New England Ultraviolet Co., USA) with an overall radiation intensity of 2.5 mW cm<sup>-2</sup>.

### 2.5 Catalyst characterisation

The Pt/TiO<sub>2</sub> samples were analysed by atomic absorption spectrometry (AAS). AAS analyses were carried out with a Solaar M6 Unicam Atomic Absorption (Rochester, USA). Additionally, determination of parameters of the porous structure was made. The surface area of obtained powders

was measured using low-temperature N<sub>2</sub> sorption (ASAP 2020 analyser, Micromeritics Instrument Co.). All powders were degassed at 120 °C for 4 h before measurement. The surface area value was determined by the multipoint BET method analysing adsorption data in a relative pressure (p/p<sub>0</sub>) range of 0.06–0.30. The desorption isotherm was utilised to determine the pore size distribution as well as the total volume of pores based on the Barrett, Joyner and Halenda (BJH) method [20].

### 2.6 Photocatalytic degradation experiments

A total of 100 ml of C. I. Acid Green 25 and C. I. Basic Blue 9 suspensions (0.04 mmol dm<sup>-3</sup>) with 0.25 g dm<sup>-3</sup>, 0.50 g dm<sup>-3</sup>, or 1 g dm<sup>-3</sup> of catalysts 1-3 (Table 3) at neutral pH was prepared. Before each experiment, dye suspensions were kept in the dark for 24 h to achieve equilibrium. During this time, the absorption of the dyes fell negligibly (ca. 3%). The degradation of the dye suspensions was carried out in a Rayonet RPR-200 Photochemical Reactor equipped with eight RPR 3000A UV lamps emitting radiation of 300 nm (Southern New England Ultraviolet Co., USA) with a radiation intensity of 6.4 mW cm<sup>-2</sup>.

### 2.7 The degradation rate constants obtained in photocatalytic experiments

The degradation rate constant (k) was determined according to quasi-first-order kinetics using equation (7):

$$\ln \frac{C_0}{C} = kt \quad (7)$$

where C<sub>0</sub> is the concentration of the dye when the equilibrium state was achieved, C is the concentration at time t, and k is the reaction rate constant. All experiments were repeated at least twice (standard deviation range 2-4%). C values were calculated based on changes in absorbance (Jasco V-670, Jasco, Japan). Before absorbance measurement, samples were filtered through a 0.22 μm PTFE Millipore membrane filter to remove TiO<sub>2</sub>.

## 3. RESULTS AND DISCUSSION

### 3.1. Cyclic and differential pulse voltammograms of C. I. Acid Green 25 and C. I. Basic Blue 9 oxidation

Both cyclic (CV) and differential pulse voltammetry (DPV) were used in the electrochemical oxidation of tested dyes using platinum electrodes since the latter method exhibits better resolution and enables better separation of peaks. Examples of CV and DPV voltammograms of the dye oxidation and electrolyte (0.1 mol dm<sup>-3</sup>) at the platinum electrode are shown in Figure 2.

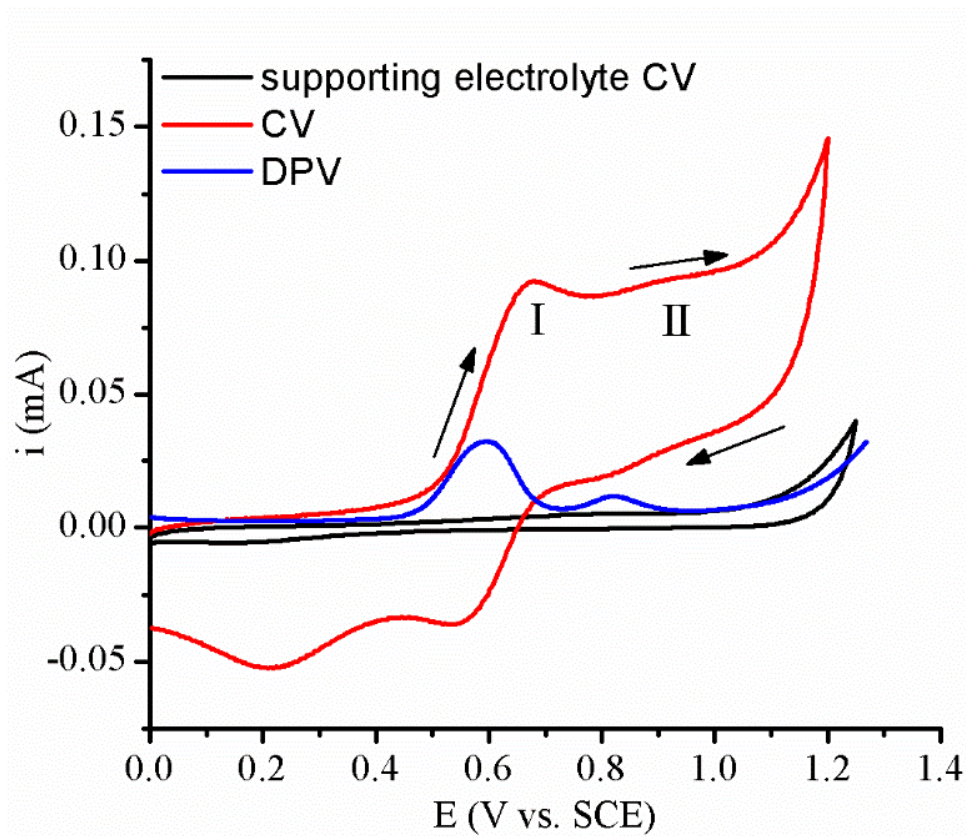


**Figure 2.** CV and DPV voltammogram of C. I. Acid Green 25 oxidation and CV voltammogram of supporting electrolyte at the platinum electrode:  $c = 1 \times 10^{-3} \text{ mol dm}^{-3}$  in  $0.1 \text{ mol dm}^{-3} \text{ NaClO}_4$ ,  $v = 0.1 \text{ V s}^{-1}$ .

It is evident that the oxidation of this dye proceeded in at least two steps and that the potential peak ( $E_{pa}$ ) from DPV responded to the half-wave potential ( $E_{1/2}$ ) obtained with the application of the CV method. Two peaks present in DPV suggest the diffusive character of dye oxidation and the lack of its adsorption on platinum. The first peak at 0.65 V is well-shaped, whereas the second at 0.88 V is rather poor. In the reverse scan, two current peaks appeared indicating the reduction of the products formed during oxidation of the dye.

To estimate the character of the electrode reaction, the dependence of the peak current ( $i_p$ ) at different concentrations of the dye on the square root of the scan rate ( $v^{1/2}$ ) and  $\ln(i_p)$  versus  $\ln(v)$  were determined. The results are presented in Figure 3.

Although Figure 3A shows the linear relationship of ( $i_p$ ) versus ( $v^{1/2}$ ), this curve does not cross the origin of the coordinates. This fact indicates that the process may be controlled either by diffusion or adsorption. For a more precise explanation of this problem, the relationship of  $\ln(i_p)$  versus  $\ln(v)$  was tested (Figure 3B), and it was found that for all dye concentrations, the slope of the curve  $\ln(i_p)$  versus  $\ln(v)$  is 0.455, indicating the diffusive character of the studied electrode reactions [21-23].

The influence of dye concentration on the oxidation reaction with the application of CV and DPV (Figure 4) at the platinum electrode was also examined.

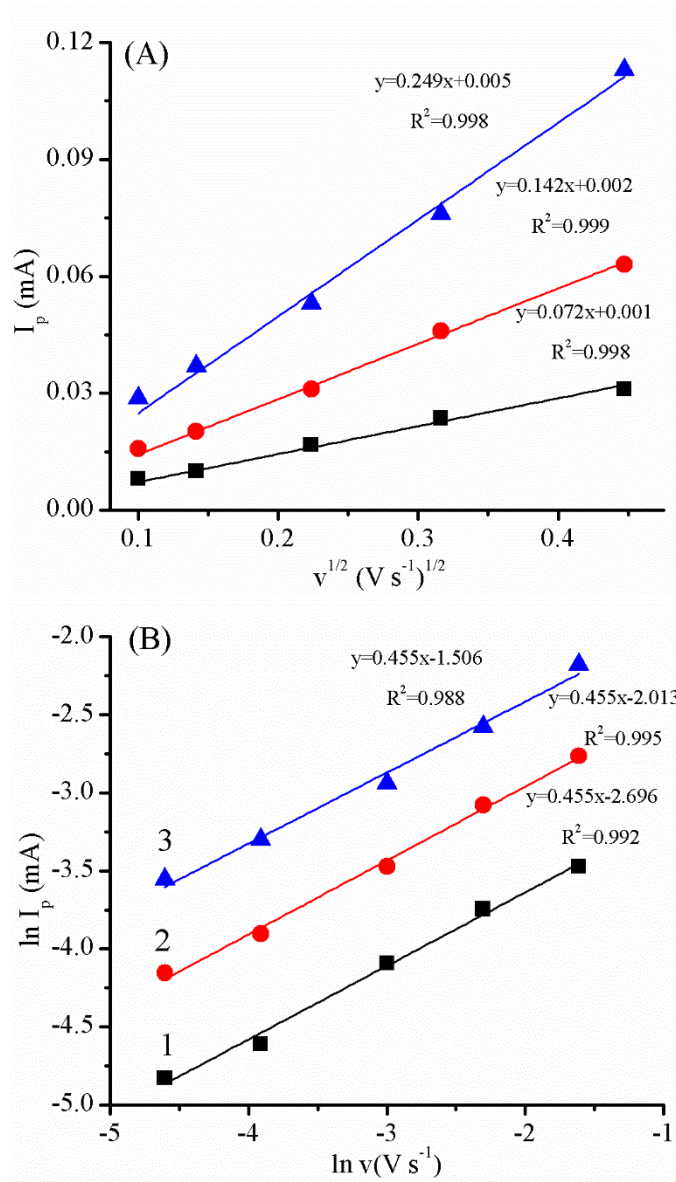


**Figure 3.** (A) Dependence of the anodic peak current ( $i_p$ ) on the square root of the scan rate ( $v^{1/2}$ ), (B) dependence of  $\ln(i_p)$  on  $\ln(v)$  in oxidation at various concentrations of C. I. Acid Green 25: 1:  $c = 0.25 \text{ mmol dm}^{-3}$ , 2:  $c = 0.50 \text{ mmol dm}^{-3}$ , 3:  $c = 1.0 \text{ mmol dm}^{-3}$ .

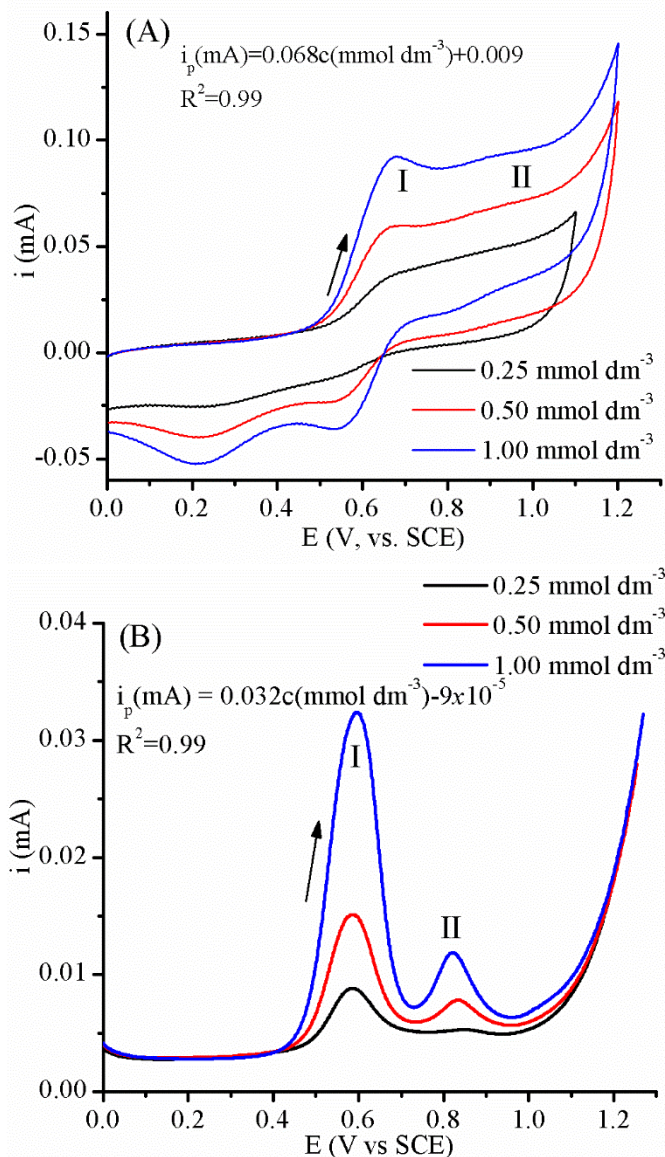


**Figure 4.** (A) CV and (B) DPV voltammograms of C. I. Acid Green 25 oxidation at the platinum electrode at different concentrations of the dye; amplitude 25 mV; pulse width 50 ms (scan rate  $0.01 \text{ V s}^{-1}$ ).

When the concentration of dye was increased, the current peak ( $i_p$ ) of dye oxidation estimated with the application of CV and DPV increased linearly as described by the equations shown in Figure 4.

In the final part of the electrochemical study of C. I. Acid Green 25 oxidation, due to an expected synergy effect, titanium electrodes coated with  $\text{TiO}_2(70\%)/\text{RuO}_2(30\%)$  and  $\text{TiO}_2(97\%)/\text{RuO}_2(3\%)$  were tested. Examples of C. I. Acid Green 25 oxidation carried out with the application of different electrode materials are presented in Figure 5.

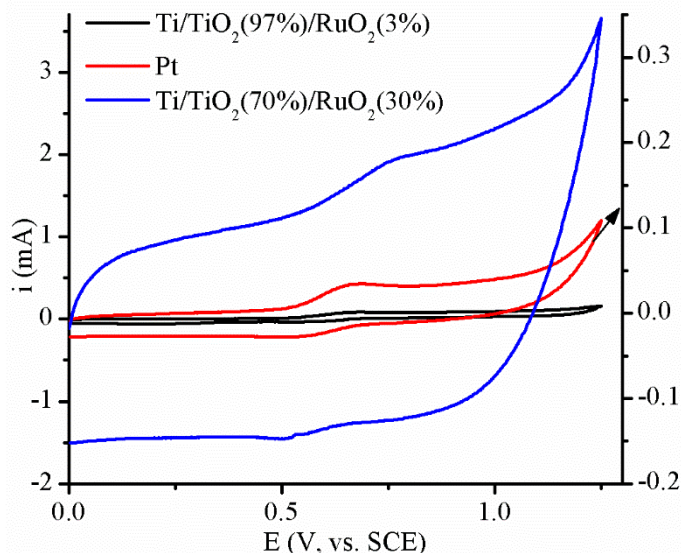


**Figure 5.** Cyclic voltammograms of C. I. Acid Green 25 oxidation recorded at different electrode materials;  $c = 1.0 \text{ mmol dm}^{-3}$  in  $0.1 \text{ mol dm}^{-3} \text{ NaClO}_4$ ,  $v = 0.1 \text{ Vs}^{-1}$ .

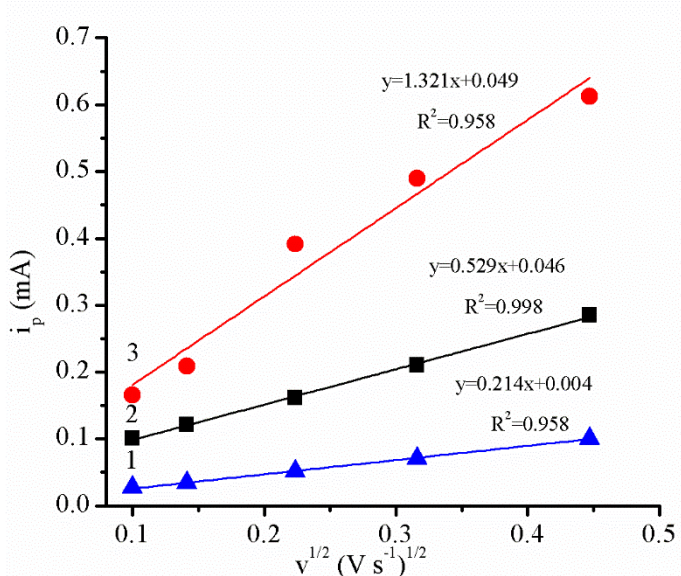


**Figure 6.** Dependence of the anodic peak current ( $i_p$ ) on the square root of the potential scan rate ( $v^{1/2}$ ) for C. I. Acid Green 25 oxidation recorded at different electrodes: 1: Pt, 2:  $\text{Ti/TiO}_2(97\%)/\text{RuO}_2(3\%)$ , 3:  $\text{Ti/TiO}_2(70\%)/\text{RuO}_2(30\%)$   $c = 1.0 \text{ mmol dm}^{-3}$  in  $0.1 \text{ mol dm}^{-3} \text{ NaClO}_4$ .

Oxidation of the dye at  $\text{Ti/TiO}_2/\text{RuO}_2$  electrodes proceeded in at least one step before the potential reached the value at which oxygen evolution began and was irreversible. The current of the first oxidation step depended on the electrode used, the lowest being for platinum and the highest for titanium coated with  $\text{TiO}_2(70\%)/\text{RuO}_2(30\%)$ . In addition, at the titanium electrode coated with the mixture of  $\text{TiO}_2/\text{RuO}_2$ , the oxidation of the dye started at 0.03-0.05 V higher than at the platinum

electrode, which indicates that the application of Ti/TiO<sub>2</sub>/RuO<sub>2</sub> electrodes made this process thermodynamically more difficult. However, the oxygen evolution was higher.

Again, in order to estimate the character of the electrode reaction, the dependences of the peak current ( $i_p$ ) in C. I. Acid Green 25 oxidation with different materials on the square root of the scan rate ( $v^{1/2}$ ) and  $\ln(i_p)$  versus  $\ln(v)$  were determined. The results are presented in Figures 6 and 7.

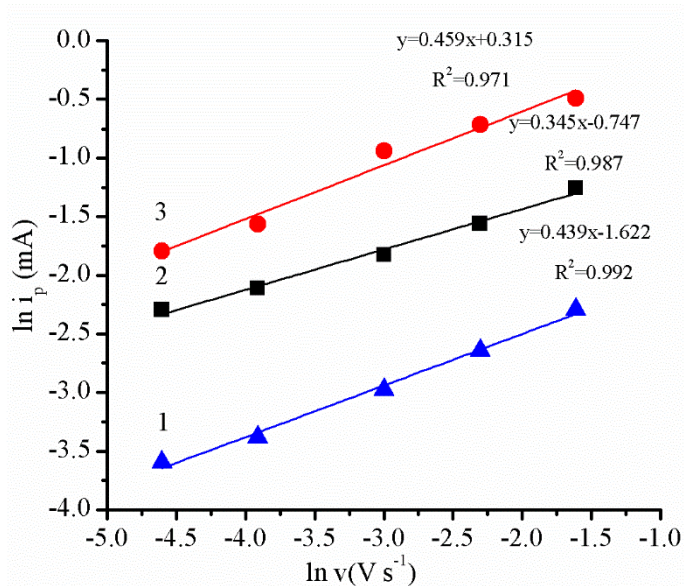
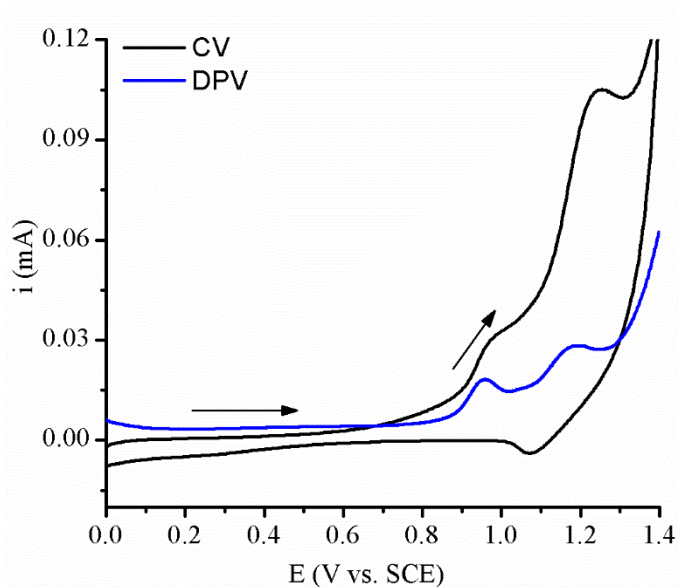


**Figure 7.** Dependence of  $\ln(i_p)$  on  $\ln(v)$  for C. I. Acid Green 25 oxidation recorded at different electrodes: 1: Pt, 2: Ti/TiO<sub>2</sub>(97%)/RuO<sub>2</sub>(3%), 3: Ti/TiO<sub>2</sub>(70%)/RuO<sub>2</sub>(30%);  $c = 1.0 \text{ mmol dm}^{-3}$  in  $0.1 \text{ mol dm}^{-3} \text{ NaClO}_4$ .

The slopes of  $\ln(i_p)$  versus  $\ln(v)$  of dye oxidation at platinum, Ti/TiO<sub>2</sub>/RuO<sub>2</sub>(97%/3%) and Ti/TiO<sub>2</sub>/RuO<sub>2</sub>(70%/30%) electrodes are 0.439, 0.345 and 0.459, respectively, which indicates that the process is diffusion-controlled.

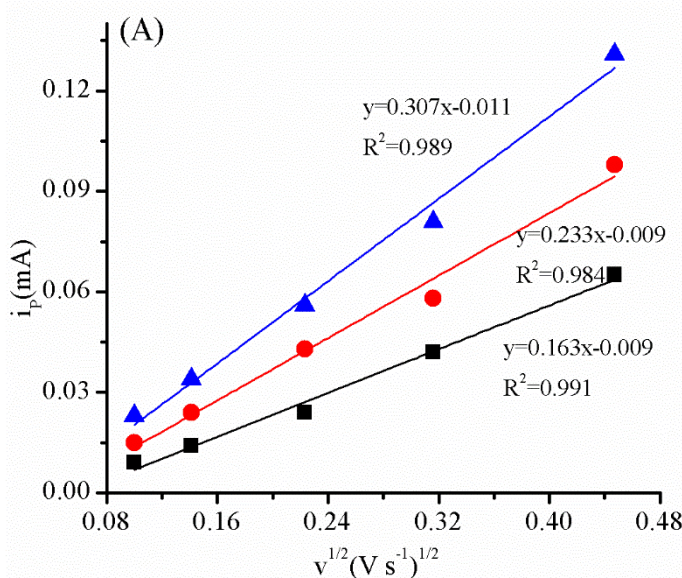
The same electrochemical studies were carried out for C. I. Basic Blue 9 with the exception of the electrolyte used (KCl) due to the lack of dye solubility in NaClO<sub>4</sub>. Figures 8 - 12 illustrate the results of all measurements from which the following conclusions may be drawn:

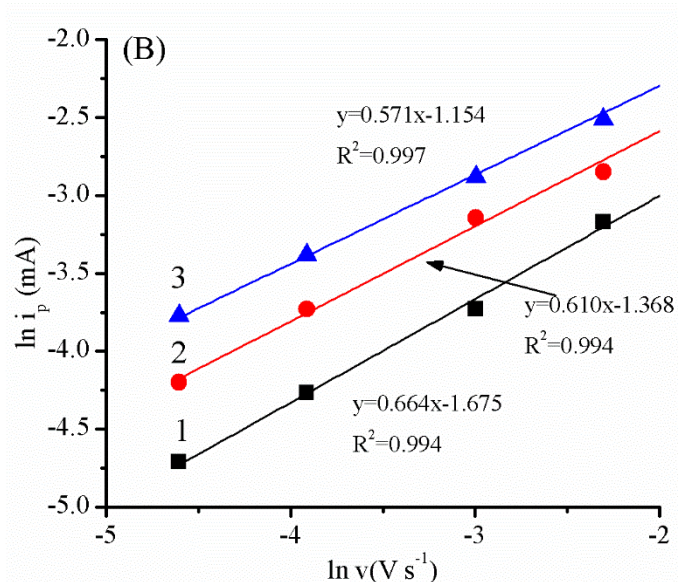
- the oxidation of C. I. Basic Blue 9 proceeded at platinum in at least two steps before the potential reached the value at which oxygen evolution began (Figure 8). Two peaks were present in the voltammograms - the first one at 0.98 V and the second at 1.18 V. In the reverse scan, one current peak appeared suggesting the reduction of the products formed during oxidation of the dye.



**Figure 8.** CV and DPV voltammogram of C. I. Basic Blue 9 oxidation at the platinum electrode:  $c = 1 \times 10^{-3} \text{ mol dm}^{-3}$  in  $0.1 \text{ mol dm}^{-3} \text{ KCl}$ ,  $v = 0.01 \text{ V s}^{-1}$ .

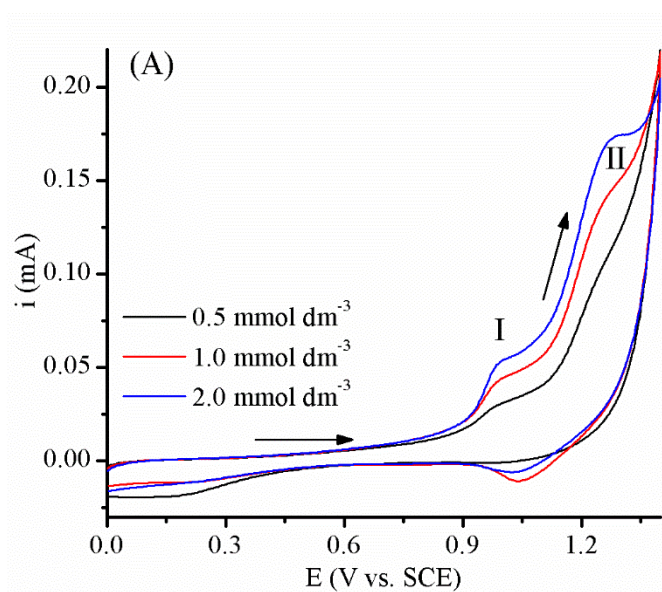
- the relationship of the peak current ( $i_p$ ) at different concentrations of the dye on the square root of the scan rate ( $v^{1/2}$ ) and  $\ln(i_p)$  versus  $\ln(v)$  at the platinum electrode showed linearity (Figure 9). In both cases, the curves did not cross the origin of the coordinates. As shown in Figure 9B, the slope of the line changed with increased dye concentration (0.664-0.571), suggesting that the process was adsorption-diffusion controlled.





**Figure 9.** (A) Dependence of the anodic peak current ( $i_p$ ) on the square root of the scan rate ( $v^{1/2}$ ), (B) dependence of  $\ln(i_p)$  on  $\ln(v)$  in oxidation at various concentrations of C. I. Basic Blue 9: 1:  $c = 0.5 \text{ mmol dm}^{-3}$ , 2:  $c = 1.0 \text{ mmol dm}^{-3}$ , 3:  $c = 2.0 \text{ mmol dm}^{-3}$ .

- the study of the influence of dye concentration with the application of CV and DPV at the platinum electrode (Figure 10) showed that at higher dye concentrations, the current peak ( $i_p$ ) became higher. Due to the diffusive-adsorptive character of the electrode reaction, the CV method was not suitable for dye concentration determination.



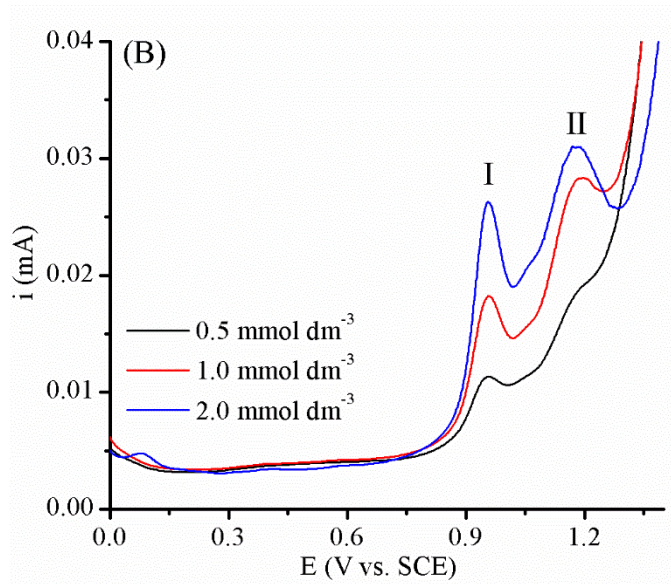


**Figure 10.** (A) CV and (B) DPV voltammograms of C. I. Basic Blue 9 oxidation at the platinum electrode at different concentrations of the dye; amplitude 25 mV; pulse width 50 ms (scan rate  $0.01 \text{ V s}^{-1}$ ).

- the oxidation of dye at the  $\text{Ti/TiO}_2/\text{RuO}_2$  electrode proceeded irreversibly in one step before the potential reached the value at which oxygen evolution began (Figure 11). The current density of the first oxidation step depended on the electrode used, with the lowest being with the platinum electrode and the highest with the titanium electrode coated with  $\text{TiO}_2/\text{RuO}_2$ . Additionally, in the latter case, the evolution of oxygen was higher.

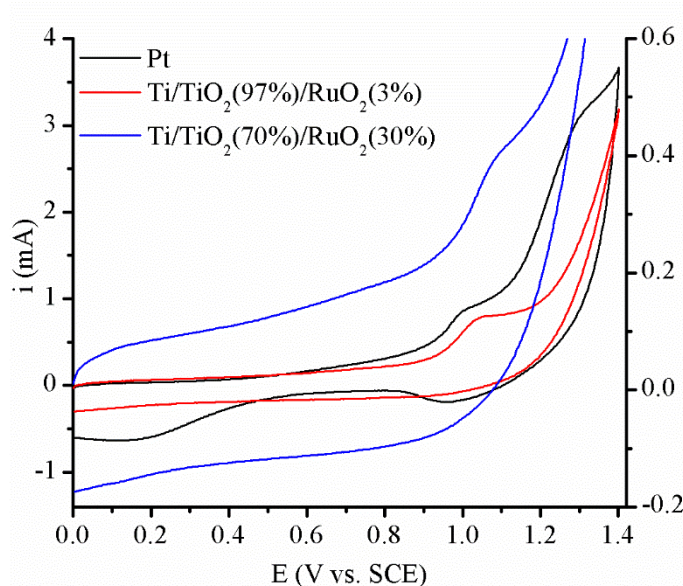


**Figure 11.** Cyclic voltammograms of C. I. Basic Blue 9 oxidation recorded at different electrode materials;  $c = 1.0 \text{ mmol dm}^{-3}$  in  $0.1 \text{ mol dm}^{-3} \text{ KCl}$ ,  $v = 0.1 \text{ Vs}^{-1}$ .

- the dependence of  $\ln(i_p)$  as a function of  $\ln(v)$  indicates that the process was adsorption-diffusion controlled (Figure 12).

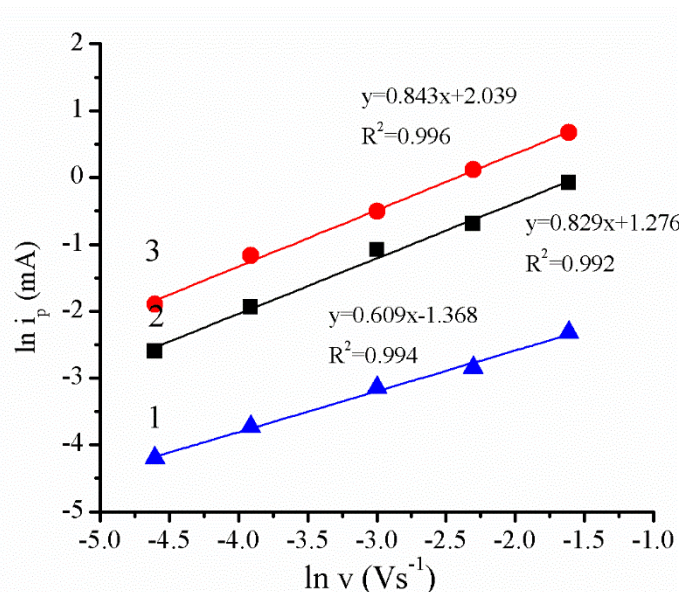


**Figure 12.** Dependence of  $\ln(i_p)$  on  $\ln(v)$  for C. I. Basic Blue 9 oxidation recorded at different electrodes: 1: Pt, 2: Ti/TiO<sub>2</sub>(97%)/RuO<sub>2</sub>(3%), 3: Ti/TiO<sub>2</sub>(70%)/RuO<sub>2</sub>(30%);  $c = 1.0 \text{ mmol dm}^{-3}$  in  $0.1 \text{ mol dm}^{-3}$  KCl.

**Table 1.** Half-wave potential ( $E_{1/2}$ ), peak current ( $i_p$ ), anodic transition coefficient ( $\beta_n\beta$ ) and heterogeneous rate constant ( $k_{bh}$ ) values for the first step of C. I. Acid Green oxidation;  $c = 1.0 \text{ mmol dm}^{-3}$  in  $0.1 \text{ mol dm}^{-3}$  NaClO<sub>4</sub> and C. I Basic Blue 9 oxidation;  $c = 1.0 \text{ mmol dm}^{-3}$  in  $0.1 \text{ mol dm}^{-3}$  KCl.

Electrode	$E_{1/2}$ (V) <sup>a</sup>	$i_p \times 10^4$ (A) <sup>a</sup>	$\beta_n\beta^a$	$k_{bh} \times 10^4$ (cm s <sup>-1</sup> ) <sup>a</sup>	$E_{1/2}$ (V) <sup>b</sup>	$i_p \times 10^4$ (A) <sup>b</sup>	$\beta_n\beta^b$	$k_{bh} \times 10^4$ (cm s <sup>-1</sup> ) <sup>b</sup>
Pt	0.62	0.71	0.59	2.78	0.97	0.58	0.98	2.22
Ti/TiO <sub>2</sub> /RuO <sub>2</sub> (97% /3%)	0.65	2.10	0.59	2.84	1.01	4.99	0.91	2.59
Ti/TiO <sub>2</sub> RuO <sub>2</sub> (70% /30%)	0.67	4.91	0.76	3.12	1.02	11.20	0.92	2.98

<sup>a</sup>AG, <sup>b</sup>MB

Since the electrochemical process occurred under diffusion-controlled conditions in the case of C. I. Acid Green 25 ( $v = 0.1 \text{ V s}^{-1}$ ) and under adsorption-diffusion-controlled conditions in the case of C. I. Basic Blue ( $v = 0.01 \text{ V s}^{-1}$ ), the anodic transition coefficient ( $\beta_n\beta$ ) and heterogeneous rate constant ( $k_{bh}$ ) were calculated. The heterogeneous rate constant ( $k_{bh}$ ) determined for a specified potential,  $E$ , characterises the transfer rate of electrons through the electrode-solution interface, whereas the electron

transition coefficient characterises the symmetry of the activated barrier of an electrode reaction. The other parameters were determined from recorded voltammograms.

The overall results regarding the electrochemistry of C. I. Acid Green 25 and C. I. Basic Blue 9 are summarised in Table 1.

The results obtained showed that the oxidation of both dyes proceeded easier at the platinum electrode. However, the peak current ( $i_p$ ) and the heterogeneous rate constant ( $k_{bh}$ ) for the first step of dye oxidation at both electrodes coated with  $TiO_2/RuO_2$  (70%/30%) were the highest: therefore, in further photoelectrochemical experiments, the latter electrode was used.

### 3.2. Electrochemical (electrolysis) and photoelectrochemical (photoelectrolysis) treatment of the dyes

In the next step, following the procedure similar to that adopted previously [24], the electrolysis of the tested dyes was carried out using the conditions corresponding to a current density of  $2.0 \times 10^{-2} A cm^{-2}$  (the current intensity = 0.4 A, the electrode surface is  $20 cm^2$ ). During preliminary investigation, it was found that the reasonable substrate conversion calculated as a change in the absorbance was achieved when the electrolyses were carried out within 1.5 h at room temperature. To increase the yield of C. I. Acid Green 25 and C. I. Basic Blue 9 conversion, a combined electrochemical (with the application of the titanium electrode coated with a mixture of  $TiO_2$  and  $RuO_2$ ) and photochemical process was conducted using the parameters applied in a single electrochemical process. The results of these experiments including UV irradiation are shown in Table 2.

**Table 2.** Dependence of C. I. Acid Green 25 and C. I. Basic Blue 9 degradation on the type of process

Process type	AG	AG	AG	MB	MB	MB
	conversion $\eta_{TOC}$ (%) <sup>a</sup>	conversion $\eta_{COD}$ (%) <sup>b</sup>	conversion $\eta_{Abs}$ (%) <sup>c</sup>	conversion $\eta_{TOC}$ (%) <sup>a</sup>	conversion $\eta_{COD}$ (%) <sup>b</sup>	conversion $\eta_{Abs}$ (%) <sup>c</sup>
Electrolysis	15.4	20.0	71.2	77.3	not determined	100.0
UV irradiation (254 nm)	11.1	10.0	30.1	19.2	20.0	50.9
UV irradiation (300 nm)	15.6	10.0	6.0	4.2	16.2	8.5
UV irradiation (350 nm)	none	none	none	none	none	none
Photo- assisted electrolysis (254 nm)	43.7	60.0	99.2	86.7	not determined	100.0
Photo- assisted electrolysis (300 nm)	15.7	30.0	70.1	77.3	not determined	100.0
Photo- assisted electrolysis (350 nm)	15.0	10.0	70.0	72.5	not determined	100.0

The concentration of the dyes is  $0.04 \text{ mmol dm}^{-3}$ , initial pH=7.0; current density =  $2.0 \times 10^{-2} \text{ cm}^{-2}$ ; temperature  $20 \text{ }^\circ\text{C}$ ; electrolysis, photolysis and photoassisted electrolysis duration - 1.5 h; electrolyte =  $0.1 \text{ mol dm}^{-3} \text{ NaClO}_4$  (AG),  $0.1 \text{ mol dm}^{-3} \text{ KCl}$  (MB), volume solution = 100 ml; a, b, c conversion of the dyes presented as a change in TOC ( $\eta_{\text{TOC}}$ ), in COD ( $\eta_{\text{COD}}$ ) and in absorbance ( $\eta_{\text{Abs}}$ ).

Table 2 shows that a single electrochemical oxidation of C. I. Acid Green 25 resulted in approximately 71% decolourisation after 1.5 h of treatment, whereas the substrate was only partly decolourised (30%) with the influence of 254 nm light within the same time. On the other hand, when photoassisted electrolysis with the use of 254 nm light was applied, the conversion of the dye was almost complete. Our study also showed that the conversion of AG estimated as a change in TOC and COD strongly depended on the experimental conditions. The simple electrochemical treatment of AG resulted in approximately 15% TOC and 20% COD removal, whereas 254 nm light caused only ca. 11% and 10% conversion of the dye based on TOC and COD removal, respectively. However, when the combined procedure was applied, the conversion of the dye increased to approximately 44% and 60% in terms of  $\eta_{\text{TOC}}$  and  $\eta_{\text{COD}}$ . From the comparison of corresponding parameters shown in Table 2, it is evident that the synergistic effect between both processes existed upon 254 nm light irradiation. The well-known synergy is explained as follows [14]. First, high energy photons (254 nm) additionally contribute to the diminution of the electron-hole pair recombination from excited  $\text{TiO}_2$  enabling the formation of hydroxyl radicals  $\text{OH}\cdot$  and second, the electrocatalytic activity of  $\text{RuO}_2$  coupled with oxygen evolution is favourable for the photochemical process because the superoxides  $\text{O}_2^{\cdot-}$  produce additional powerful oxidants (radicals  $\text{OH}\cdot$ ), enhancing degradation of the organic substrate. The photochemical processes that occur are shown below [14]:



It is worth mentioning, that there are new papers published, concerning the degradation of C. I. Acid Green 25. An example is electrochemical degradation with the application of lead oxide coated titanium anode in the presence of sodium chloride [25]. However, the data presented here cannot be compared with our results due to quite different conditions used: i.e. different initial dye concentration, higher temperature, acidic pH and different electrolyte-NaCl. In this case, electrogenerated  $\text{Cl}_2$ , from NaCl, participates in  $\text{ClO}^-$  ions formation which enhanced the degradation of the dye. On the other hand, when the process was conducted in the absence of chloride containing electrolytes, the efficiency of the dye and COD removal was low. This shows, that the degradation of C. I. Acid Green 25 achieved in our experiments (photoassisted electrolysis) resulted in very good colour, COD and additionally TOC removal. Another, interesting approach to the degradation of C. I. Acid Green 25 was presented in [26]. In this paper, the evaluation of operational parameters using statistical method (response surface methodology) was reported. The results obtained were very good.

Summarising the results obtained for C. I. Basic Blue 9 (Table 2), the following conclusions were drawn. When the single electrochemical process was applied, the decolourisation of the dye was complete, while the single photochemical treatment with 254 nm light resulted in ca. 50% decolourisation. Moreover, single electrochemical oxidation resulted in approximately 77% TOC removal, whereas 254 nm light caused only 19.2% and 20% conversion of the dye based on TOC and COD removal, respectively. Although in this case the synergistic effect in photoassisted electrolysis was difficult to observe (due to complete decolourisation occurring in the single electrolysis process and the lack of COD determination), very high (86.7%) mineralisation of the dye based on TOC was achieved. In this place, it is worth mentioning that nowadays C. I. Basic Blue 9 is widely used in medicine and biology (bacteriology, as an oxidation-reduction indicator, as an antidote to cyanide and as antiseptic in veterinary domain). Its application in textile industry is rather limited. However, due to its easy accessibility, it became recently common model object for testing the efficiency of new electrochemical and photoelectrochemical procedures. In the study [27] the direct and indirect electrochemical oxidation of MB was performed under different conditions. Therefore, the results presented here cannot be compared to our results. On the other hand, very interesting results were obtained when photoelectrochemical degradation of C. I. Basic Blue 9 with the application of  $\beta$ -PbO<sub>2</sub> electrode was carried out [28]. This electrode exhibited not only high photoactivity under the influence of visible light, but also a significant synergy effect in photoelectrochemical process. However, only kinetics parameters of this process were reported. Synergy was also observed in photoelectrochemical degradation of Methylene Blue, when three-dimensional electrode-photocatalytic reactor was used [29]. In this case, comparable results in terms of decolouration and TOC removal were achieved and the process was very fast (30 min).

### 3.3 Photocatalytic treatment of the dyes

The next part of our research was extended to the photocatalytic treatment of the organic dyes with the application of P25 and Pt/P25 catalyst in order to compare the effectiveness of the procedures used. The Pt/TiO<sub>2</sub> samples were analysed by atomic absorption spectrometry (AAS), and the content of platinum was estimated. Although the content of platinum was found to be slightly lower than expected (Table 3), in the subsequent discussion, the theoretical content was always used.

**Table 3.** AAS analysis of Pt content in Pt/P25 catalysts

Name Pt/P25	Theoretical Pt content wt. %	Measured Pt content wt. %
Catalyst 1	0.15	0.09
Catalyst 2	0.30	0.29
Catalyst 3	0.50	0.42

In addition, the textural properties of P25 and Pt/P25 samples were investigated by low-temperature N<sub>2</sub> sorption isotherms (Figure 13).

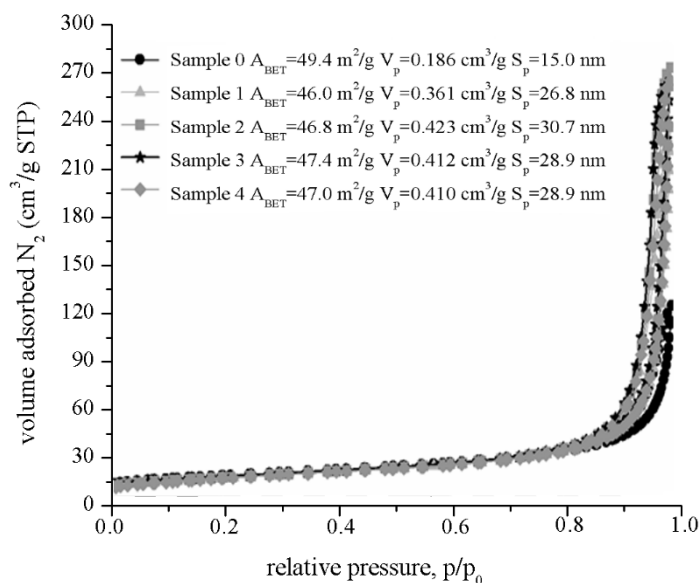


**Figure 13.** N<sub>2</sub> adsorption/desorption isotherms of Pt and Pt/P25 samples

Sample 0 is P25, whereas samples 1, 2 and 3 represent catalysts 1–3 obtained under the influence of 575 nm light. For comparison, sample 4 was also characterised, which is 0.50 wt.% Pt/P25 obtained with the application of 300 nm light.

The isotherms measured for commercial P25 and P25 modified with Pt were classified as type IV with hysteresis loops of H1 type, suggesting their mesoporous structure and cylindrical pore geometry. The amount of nitrogen adsorbed gently increased in the relative pressure range  $p/p_0=0-0.8$ ; and above this, a rapid increase was observed, which resulted in the maximum amount of adsorbed nitrogen at  $p/p_0=0.99$ . Commercial titanium dioxide (sample 0) has the highest surface area (BET), equal to  $49.4 \text{ m}^2 \text{ g}^{-1}$ . The mean pore diameter of this powder is 15 nm, and the total pore volume is  $0.186 \text{ cm}^3 \text{ g}^{-1}$ . Samples of P25 modified with Pt exhibit quite similar parameters of the porous structure. The surface area of those samples is in the range of  $46.0-47.4 \text{ m}^2 \text{ g}^{-1}$ , the mean pore diameter is in the range of 26.8–30.7 nm, and the total pore volume is in the range of  $0.361-0.423 \text{ cm}^3 \text{ g}^{-1}$ . Only a slight decrease in surface area compared to P25 was noted. On the other hand, significant changes were observed when analysing the pore volume and diameters. Increasing both, the  $S_p$  and  $V_p$  parameters suggest that Pt species are probably located in the interior of the pores resulting in their swelling. Some may also be attached to the active sites present on the titanium surface, as evidenced by the slightly lower values of ABET within respect to pure TiO<sub>2</sub> [30, 31]. Among the Pt/P25 materials obtained, the largest surface area of 47.4 and  $47.0 \text{ m}^2 \text{ g}^{-1}$  was noted for samples 3 and 4, respectively. The mean pore diameter of the mentioned materials was 28.9 nm, and the total pore volume was  $0.412 \text{ cm}^3 \text{ g}^{-1}$  (sample 3) and  $0.410 \text{ cm}^3 \text{ g}^{-1}$  (sample 4). The lowest value of ABET ( $46.0 \text{ m}^2 \text{ g}^{-1}$ ) was recorded for sample 1. This sample has a pore volume of  $0.361 \text{ cm}^3 \text{ g}^{-1}$  and a pore diameter of 26.8 nm.

To analyse the progress of dyes degradation several series of tests were performed. In all tests the concentration of the dyes was constant i.e. at  $0.04 \text{ mmol dm}^{-3}$ , whereas the concentration of catalyst was kept at the level 0.25, 0.50,  $1 \text{ g dm}^{-3}$  and additionally different content of Pt in catalyst was present in each case (0.15 wt%, 0.30 wt%, 0.50 wt%). A large number of experiments led us to some generalisation about the optimal operative conditions. We assumed that reasonable, from economical point of view, results were obtained for catalysts at their  $0.50 \text{ g dm}^{-3}$  concentration. Figures 14 and 15 illustrate the representative degradation profiles for C. I. Acid Green 25 and C. I. Basic Blue 9. It is evident that the degradation curves of AG and MB by Pt/TiO<sub>2</sub> catalyst were well fitted by a mono-exponential curve suggesting that a pseudo-first order reaction model can be used to describe the kinetic behaviour of these dyes. The detailed rate constants of both substrates degradation in the presence of P25 and catalysts 1-3 with different Pt content in 100 ml suspension containing  $0.50 \text{ g dm}^{-3}$  of the catalyst are shown in Table 4.

To analyse the progress of dye degradation, several tests were performed. In all tests, the concentration of the dye was constant, i.e. at  $0.04 \text{ mmol dm}^{-3}$ , whereas the concentration of catalyst was kept at the level of 0.25, 0.50, or  $1 \text{ g dm}^{-3}$ , and additionally, different contents of Pt in the catalyst were present in each case (0.15 wt%, 0.30 wt%, and 0.50 wt%). A large number of experiments led us to some generalisations about the optimal operative conditions. We assumed that reasonable, from an economical point of view, results were obtained for catalysts at their  $0.50 \text{ g dm}^{-3}$  concentration. Figures 14 and 15 illustrate the representative degradation profiles for C. I. Acid Green 25 and C. I. Basic Blue 9. It is evident that the degradation curves of AG and MB by Pt/TiO<sub>2</sub> catalyst were well fitted by a mono-exponential curve suggesting that a pseudo-first-order reaction model can be used to describe the kinetic behaviour of these dyes. The detailed degradation rate constants of both substrates in the presence of P25 and catalysts 1-3 with different Pt contents in a 100 ml suspension containing  $0.50 \text{ g dm}^{-3}$  of the catalyst are shown in Table 4.

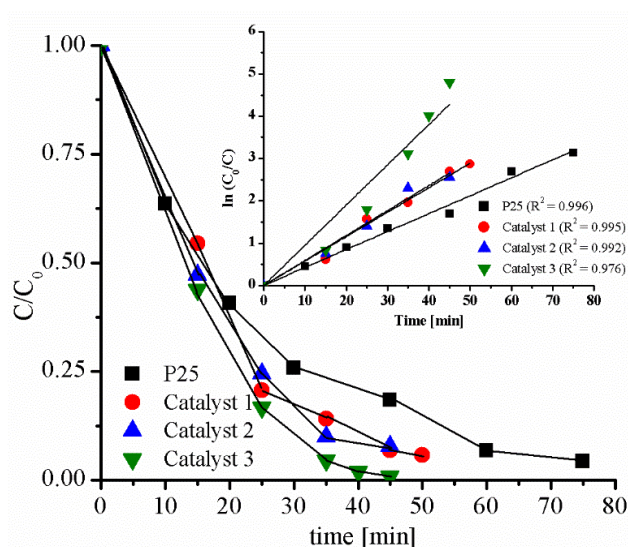


**Figure 14.** The degradation profiles of C. I. Acid Green 25 ( $0.04 \text{ mmol dm}^{-3}$ ) in the presence of P25 and catalysts 1-3 used at the concentration of  $0.50 \text{ g dm}^{-3}$ .

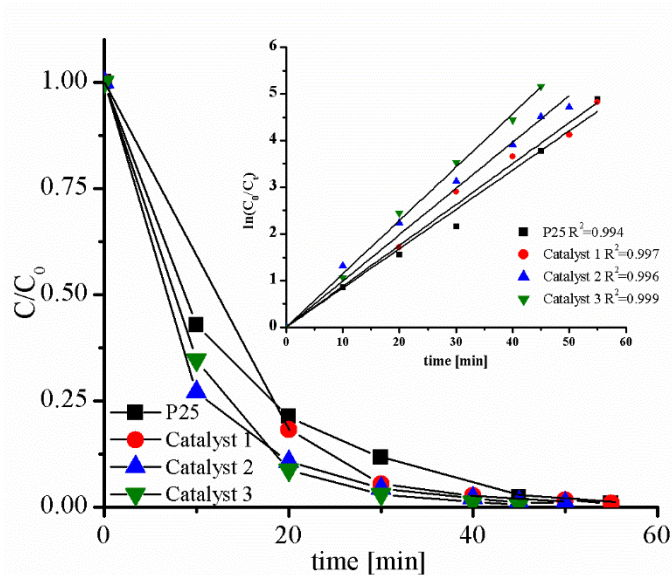


**Figure 15.** The degradation profiles of C. I. Basic Blue 9 ( $0.04 \text{ mmol dm}^{-3}$ ) in the presence of P25 and catalysts 1-3 used at the concentration of  $0.50 \text{ g dm}^{-3}$ .

**Table 4.** Rate constants calculated from the insets of Figures 14 and 15 for the degradation of C. I. Acid Green 25 and C. I. Basic Blue 9

Catalyst	$k \times 10^3$ [s <sup>-1</sup> ] <sup>a</sup>	R <sup>2a</sup>	$k \times 10^3$ [s <sup>-1</sup> ] <sup>b</sup>	R <sup>2b</sup>
P25	0.71	0.99	1.40	0.99
Catalyst 1	0.95	0.99	1.46	0.99
Catalyst 2	1.01	0.99	1.69	0.99
Catalyst 3	1.59	0.99	1.91	0.99

<sup>a</sup>AG, <sup>b</sup>MB

It can be seen (Table 4, Figures 14 and 15) that an elevated Pt content in the catalyst increased the degradation rate constants of the dyes and diminished the time needed for their total elimination. However, only a small improvement of the kinetic parameters was observed in all Pt/P25 catalysts compared with P25, especially in the case of C. I. Basic Blue 9. Our observation is consistent with the results presented in the literature previously [32, 33] for the degradation of dimethylphthalate or phenol conducted in the presence of Pt/P25. It is evident that the presence of platinum, despite its broadly discussed role, did not always provide significant benefit in the application of photocatalytic degradation. According to the abovementioned papers, platinumised P25 cannot further increase the efficiency of charge separation since this separation is already optimised by the junction between phases present in P25, where holes move into rutile and electrons are left in anatase [33].

Finally, the conversion of the tested dyes estimated as the change in the absorbance, TOC and COD was examined, and the results obtained are shown in Table 5. The extent of mineralisation of AG

and MB achieved was approximately 89-96%. This high mineralisation might be the result of the oxidation state of metallic platinum. It is worthy to mention that P25 alone did not show a high mineralisation effect. Comparing the effectiveness of the dyes decolourisation and mineralisation using photocatalytic and photoelectrochemical procedures (254 nm), the former procedure appeared to be more promising for C. I. Acid Green 25 effluent treatment in which the best conversion of the dye in terms of all analysed parameters ( $\eta_{\text{Abs}}$ ,  $\eta_{\text{TOC}}$ ,  $\eta_{\text{COD}}$ ) along with a doubled rate constant of dye decolourisation in the comparison with P25 were found. However, this is not the case for C. I. Basic Blue 9 for which comparable results were obtained when photoassisted electrolysis (254 nm) was used. In addition, the application of Pt/P25 caused a very small increase in the decolourisation rate constant over P25 alone. Therefore, it seems reasonable, due to the high price of Pt, to consider each dye individually.

**Table 5.** Dependence of C.I. Acid Green 25 and C. I. Basic Blue 9 conversion on the photocatalytic process

Name	AG conversion	AG conversion	AG conversion	MB conversion	MB conversion	MB conversion
Pt/P25	$\eta_{\text{TOC}}$ (%) <sup>a</sup>	$\eta_{\text{COD}}$ (%) <sup>b</sup>	$\eta_{\text{Abs}}$ (%) <sup>c</sup>	$\eta_{\text{TOC}}$ (%) <sup>a</sup>	$\eta_{\text{COD}}$ (%) <sup>b</sup>	$\eta_{\text{Abs}}$ (%) <sup>c</sup>
Catalyst 1	63.2	23.5	100.0	9.1	21.0	100.0
Catalyst 2	77.8	92.3	100.0	75.4	94.8	100.0
Catalyst 3	90.0	96.2	100.0	89.4	95.6	100.0

The concentration of catalyst is  $0.50 \text{ g dm}^{-3}$ ; the initial concentration of the dyes is  $0.04 \text{ mmol dm}^{-3}$ ; <sup>a, b, c</sup> conversion of the dyes presented as a change in TOC ( $\eta_{\text{TOC}}$ ), in COD ( $\eta_{\text{COD}}$ ) and in absorbance ( $\eta_{\text{Abs}}$ ).

In the end of this paper, we would like to pertain to recently published study [34] in which the preparation of  $\text{TiO}_2\text{-ZnO}$  binary oxide systems were reported. Using these catalysts the extent of MB removal was in the range ca. 81-97% after 60-120 minutes. However, the other parameters such as TOC and COD were not reported here.

#### 4. CONCLUSIONS

Very high mineralisation of studied dyes was achieved when photoassisted electrolyses and photocatalytic oxidation methods were used. Electrolyses were performed at Pt and  $\text{Ti/TiO}_2/\text{RuO}_2$  (70%/30%) electrodes. In the latter case, the oxidation of C. I. Acid Green 25 proceeded in one step before the potential reached the value at which oxygen evolution began and was irreversible. The electrode process was diffusion-controlled. The oxidation of C. I. Basic Blue 9 proceeded irreversibly in one step at  $\text{Ti/TiO}_2/\text{RuO}_2$  (70%/30%) electrodes. The electrode process was adsorption-diffusion-controlled. Although the oxidation of both dyes at the platinum electrode proceeded at lower  $E_{1/2}$ , the peak current ( $i_p$ ) and heterogeneous rate constant ( $k_{\text{bh}}$ ) for the first step of their degradation were higher when the  $\text{Ti/TiO}_2/\text{RuO}_2$  (70%/30%) electrode was employed. The satisfactory degradation of dyes was achieved when electrolyses were carried out under the conditions corresponding to the current density

of  $2.0 \times 10^{-2} \text{ A cm}^{-2}$  within 1.5 h at ambient temperature. The photoassisted (254 nm) electrochemical oxidation considerably improved the efficiency of C. I. Acid Green 25 degradation, exhibiting the synergistic effect. The dye was degraded by 99.2%, 43.7% and 60% in terms of  $\eta_{\text{Abs}}$ ,  $\eta_{\text{TOC}}$  and  $\eta_{\text{COD}}$ , respectively. Although in the case of C. I. Basic Blue 9 the synergy was not observed in photoassisted electrochemical oxidation, very high (86.7%) mineralisation of the dye based on TOC was achieved. In the photocatalytic degradation, Pt/TiO<sub>2</sub> catalysts modified with different contents of platinum were used. Very good mineralisation of both dyes was achieved using  $0.50 \text{ g dm}^{-3}$  of the catalyst containing ca. 0.50 wt.% Pt. However, only a small improvement of the kinetic parameters was observed in all Pt/P25 catalysts compared with P25, especially in the case of C. I. Basic Blue 9.

#### ACKNOWLEDGEMENT

This work was supported by Lodz University of Technology, Faculty of Chemistry - grant W-3D/FM/44G/2016.

#### References

1. A. Kar, Y.R. Smith and V. Subramanian, *Environ. Sci. Technol.*, 43 (2009) 3260.
2. J.P. Guin, Y.K. Bhardwaj and L. Varshney, *Appl. Radiat. Isot.*, 122 (2017) 153.
3. U. Caudillo-Flores, M.J. Muñoz-Batista, A. Kubacka, J. Zárate-Medina, J.A. Cortés and M. Fernández-García, *Appl. Catal., A*, 550 (2018) 38.
4. A. Bousher, X. Shen and R.G.J. Edyvean, *Water Res.*, 31 (1997) 2084.
5. A. Fujishima, X. Zhang and D.A. Tryk, *Surf. Sci. Rep.*, 63 (2008) 515.
6. J. Zhao, C. Chen and W. Ma, *Top. Catal.*, 35 (2005) 269.
7. J. Kim, C.W. Lee and W. Choi, *Environ. Sci. Technol.*, 44 (2010) 6849.
8. H. Sun, G. Zhou, S. Liu, H.M. Ang, M.O. Tadé and S. Wang, *Chem. Eng. J.*, 231 (2013) 18.
9. K. Batalovic, N. Bundaleski, J. Radakovic, N. Abazovic, M. Mitric, R.A. Silva, M. Savic, J. Belosevic-Cavor, Z. Rakocevic and C.M. Rangelb, *Phys. Chem. Chem. Phys.*, 19 (2017) 7062.
10. J. Zhang, Y. Wu, M. Xing, S.A. Ahmed, K. Leghari and S. Sajjad, *Energy Environ. Sci.*, 3 (2010) 715.
11. A.I. del Río, M.J. Benimeli, J. Molina, J. Bonastre and F. Cases, *Int. J. Electrochem. Sci.*, 7 (2012) 13074.
12. S.J. Allen, K.Y.H. Khader and B. Murad, *J. Chem. Technol. Biotechnol.*, 62 (1995) 111.
13. K. Rajeshwar, J.G. Ibanez and G.M. Swain, *J. Appl. Electrochem.*, 24 (1994) 1077.
14. R. Pelegrini, P. Peralta-Zamora, A.R. Andrade, J. Reyes and N. Duran, *Appl. Catal. B*, 22 (1999) 83.
15. S. Ardizzzone and S. Trassati, *Adv. Colloid Interface Sci.*, 64 (1996) 173.
16. M. Seralathan, R.A. Osteryong and J.G. Osteryong, *J. Electroanal. Chem. and Interfacial Electrochem.*, 222 (1987) 69.
17. Z. Galus, *Fundamentals of electrochemical analysis*. Harwood & PWN; 1994, pp. 242, 284.
18. W. Hermanowicz, J. Dojlido, W. Dozanska, B. Koziorowski, J. Zerbe, *Fizyczno-chemiczne badanie wody i ścieków*, Arkady, Warszawa 1999, pp. 93, 333, 421.
19. J. Romao, R. Salata, S.Y. Park and G. Mul, *Appl. Catal., A*, 518 (2016) 206.
20. E.P. Barret, L.G. Joyner and P.P. Halenda, *J. Am. Chem. Soc.*, 73 (1951) 373.
21. A.K. Timbola, C.D. Souza, C. Soldi, M.G. Pizzolatti and A. Spinelli, *J. Appl. Electrochem.*, 37 (2007) 617.
22. A.J. Bard, L.R. Faulkner, *Electrochemical Methods, Fundamentals and Applications*. 2nd ed. John

- Wiley & Sons, New York, 2001, pp. 236, 503, 709.
23. C.M.A. Brett and A.M.O. Brett, *Electrochemistry: Principles, Methods, and Applications*. Oxford University Press, New York, 1993, pp. 427.
  24. A. Socha, E. Sochocka, R. Podsiadły and J. Sokołowska, *Dyes Pigm.*, 73 (2007) 390.
  25. N.M. Abu Ghalva and M.S. Abdel-Latif, *J. Iran. Chem. Soc.*, 2 (2005) 238.
  26. A.R. Khataee, M. Zarei, M. Fathinia and M.K. Jafari, *Desalination*, 268 (2011) 126.
  27. M. Panizza, A. Barbucci, R. Ricotti and G. Cerisola, *Sep. Purif. Technol.*, 54 (2007) 382.
  28. G. Li, H.Y. Yip, K.H. Wong, C. Hu, J. Qu and P.K. Wong *J. Environ.Sci.*, 23 (2011) 998.
  29. T. An, X. Zhu and Y. Xiong, *Chemosphere*, 46 (2002) 897.
  30. S. Saktivel, M.V. Shankar, M. Palanichamy, B. Arabindoo, D.W. Bahnemann and V. Murugesan, *Water Res.*, 38 (2004) 3001.
  31. A. Gołębiewska, W. Lisowski, M. Jarek, G. Nowaczyk, M. Michalska, S. Jurga, A. and Zaleska-Medynska, *Mol. Catal.*, 442 (2017) 154.
  32. E.P. Melián, E. Henriques-Cárdenes, O.G. Diaz and J.M. Doña Rodríguez, *Chem. Phys.*, 475 (2016) 112.
  33. M.C. Hidalgo, M. Maicu, J.A. Navio and G. Colón, *Catalys. Today*, 129 (2007) 43.
  34. K. Siwińska-Stefańska, A. Kubiak, A. Piasecki, J. Goscińska, G. Nowaczyk, S. Jurga and T. Jesionowski, *Materials*, 11 (2018) 841.

© 2019 The Authors. Published by ESG ([www.electrochemsci.org](http://www.electrochemsci.org)). This article is an open access article distributed under the terms and conditions of the Creative Commons Attribution license (<http://creativecommons.org/licenses/by/4.0/>).